Structural Engineering and Mechanics, Vol. 14, No. 2 (2002) 191-208
DOI: http://dx.doi.org/10.12989/sem.2002.14.2.191

Pressure-temperature limit curve for reactor vessel evaluated by ASME code

Myung Jo Jhung† and Seok Hun Kim‡

Korea Institute of Nuclear Safety, 19 Kusong-dong, Yusong-gu, Daejeon 305-338, Korea

Sung Gyu Jung‡†

Korea Power Engineering Company, Inc., 360-9 Mabuk-ri, Kusong-myon, Yongin, Kyunggi-do 449-713, Korea

(Received June 29, 2001, Accepted May 20, 2002)

Abstract. A comparative assessment study for a generation of the pressure-temperature (P-T) limit curve of a reactor vessel is performed in accordance with ASME code. Using cooling or heating rate and vessel material properties, stress distribution is obtained to calculate stress intensity factors, which are compared with the material fracture toughness to determine the relations between operating pressure and temperature during reactor cool-down and heat-up. P-T limit curves are analyzed with respect to defect orientation, clad thickness, toughness curve, cooling or heating rate and neutron fluence. The resulting P-T curves are compared each other.

Key words: pressure-temperature limit curve; fracture toughness; stress intensity factor; heat-up; cool-down; reactor vessel; ASME code.

1. Introduction

A nuclear reactor pressure vessel enclosing fuel assemblies and reactor vessel internals is the most important component because it contains massive coolant of high temperature and high pressure during operation. Therefore, it must be operating safely with a sufficient integrity during operation. It is not difficult to maintain the structural integrity during operation because a reactor vessel has very high fracture toughness in high temperature condition and also there is only a membrane stress due to internal pressure.

However, during shut-down or start-up of the plant, applied stress becomes large because of the thermal stress resulting from the temperature gradient through the vessel wall in combination with the internal pressure stress from system pressure. In this case, through-wall propagation of a relatively small crack may be caused by the combination of the pressure stress and thermal stress along with a decrease in fracture toughness due to the vessel temperature falling below its nil

† Principal Researcher
‡ Researcher
‡† Senior Researcher

ductility transition temperature. Therefore, it is necessary to define the allowable relations between operating pressure and temperature during cool-down and heat-up for the assumed crack not to propagate.

The procedure to generate P-T limit curve is suggested in Appendix G to ASME code Section III and Section XI (1998a, 1998b), which is known to be conservative in some cases. In addition, there are some differences between them, which needs to be investigated by performing a series of sensitivity analyses. The oldest plant in Korea was commissioned in 1978 and is now approaching to the design life of 30 years. It is expected to extend its operating life. In this case, a lot of work should be performed to verify the structural integrity of the reactor vessel for the safe operation beyond the design life. One of them is to guarantee enough margin for the safe window of P-T limit curve during plant start-up and shut-down.

In this study, theory of fracture mechanics for generating P-T limit curve according to ASME code is investigated and numerical procedure is developed. For the given material properties, cooling or heating rate and postulated defect, the stress distribution is obtained to calculate the stress intensity factor. Then the stress intensity factor is compared with the material fracture toughness values to determine the allowable relations between operating pressure and temperature during cool-down or heat-up. Using an analysis routine developed, P-T limit curves are generated with respect to defect orientation, clad thickness, toughness curve, cooling or heating rate and neutron fluence, and their results are compared to find general characteristics that could help designers to define an operating area of nuclear power plants.

2. Problem statement

2.1 Specification of reactor vessel

Reactor vessel employed in this analysis is one of the oldest plants in Korea, which is made of SA 508 Grade 2 Class 1 with the internal diameter of 132 inches, the wall thickness of 6.5 inches and the clad thickness of 0.125 inch. The copper and nickel contents of 0.29 and 0.68 weight % for weld material, which augment radiation embrittlement, are higher than any other plants, which implies that cooling or heating may cause through-wall propagation of a relatively small crack, threatening the safety of the plant. Also, the surveillance test results showed that there is only a

Table 1 Vessel parameters for analysis

Parameter	Unit	Value
Inner diameter of shell	inch	132
Clad thickness, minimum	inch	0.125
Vessel belt line thickness, minimum	inch	6.5
Effective flow area	ft^2	16.558
Effective coolant flow rate	lb_m/hr	65.9E6
Effective hydraulic diameter	ft	1.0358
Cu content	weight %	0.29
Ni content	weight %	0.68
Initial RT_{NDT}	^oF	–10

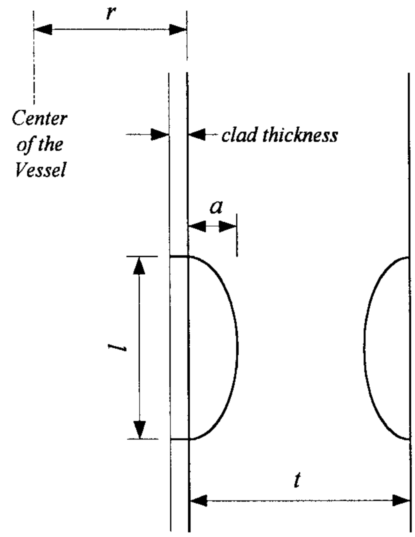

Fig. 1 Postulated defect

Table 2 Analysis matrix for pressure-temperature limit curves

Case	Direction	Clad thickness (inch)	Toughness curve, K_{IR}	Rate (°F/hr)	f_{surf} ($\times 10^{19}$ n/cm^2)
C1	Axial	0.125	K_{IA}	−100	3
C2	Axial	0.125	K_{IA}	−100	6
C3	Axial	0.125	K_{IC}	−100	3
C4	Axial	0.125	K_{IA}	−50	3
C5	Axial	0	K_{IA}	−100	3
C6	Axial	0	K_{IC}	−100	3
C7	Axial	0	K_{IA}	−50	3
C8	Circumferential	0.125	K_{IA}	−100	3
H1	Axial	0.125	K_{IA}	+100	3
H2	Axial	0.125	K_{IA}	+100	6
H3	Axial	0.125	K_{IC}	+100	3
H4	Axial	0.125	K_{IA}	+50	3
H5	Axial	0	K_{IA}	+100	3
H6	Axial	0	K_{IC}	+100	3
H7	Axial	0	K_{IA}	+50	3
H8	Circumferential	0.125	K_{IA}	+100	3

small margin in the fracture toughness. Therefore, when life extension is considered, plant specific analysis is required to assure the structural integrity of the reactor vessel. The design data of the reactor vessel used for the analysis are shown in Table 1.

The postulated defect is an inside or outside surface crack with an aspect ratio (a/l) of 1/6 and a depth ratio (a/t) of 1/4, as shown in Fig. 1.

2.2 Analytical parameters

Parametric study is performed to investigate the effect of crack direction, clad thickness, toughness curve, cooling or heating rate and neutron fluence as shown in Table 2.

The direction of defect with sharp tip is normal to the direction of maximum stress defined by ASME code Section III (1998a) and the sharp defects orient axially for plates, forgings and axial welds, and circumferentially for circumferential welds as defined by ASME code Section XI (1998b).

For the fracture assessment, two fracture toughness curves of K_{IA} and K_{IC} are assumed, which show the relationship between the reference stress intensity factor K_{IR}, ksi$\sqrt{in}$, and a temperature which is related to the reference nil ductility temperature RT_{NDT}, °F. The fracture toughness of the material is defined by two parameters K_{IA} and K_{IC}, which represent critical values of the stress intensity factors. K_{IA} is based on the lower bound of crack arrest critical K_I values measured as a function of temperature. K_{IC} is based on the lower bound of static initiation critical K_I values measured as a function of temperature. From Appendices *G* to ASME code Section III and Section XI, K_{IA} is :

$$K_{IA} = 26.78 + 1.233 \exp[0.0145\,(T - RT_{NDT} + 160)] \tag{1}$$

Also, K_{IC} endorsed by ASME code Section XI Code Case N-640 (1998c) to reduce the conservatism in the analysis is :

$$K_{IC} = 33.2 + 20.734 \exp[0.02\,(T - RT_{NDT})] \tag{2}$$

These two fracture toughness curves are used to generate P-T limit curve and the results are compared to address how much the allowable area increases by the use of K_{IC} curve.

The reference temperature of nil-ductility transition RT_{NDT} is given by USNRC (1996) as follows :

$$RT_{NDT} = RT_{NDT0} + M + \Delta RT_{NDT} \tag{3}$$

where RT_{NDT0} is the reference temperature for the unirradiated material, M (=56 °F) the margin and ΔRT_{NDT} the mean value of the adjustment in reference temperature caused by irradiation and is calculated as follows :

$$\Delta RT_{NDT} = [\mathrm{CF}] \times f^{\,0.28-0.10 \log f} \tag{4}$$

where [CF] is the chemistry factor expressed by a function of copper and nickel content, and f (10^{19} n/cm^2, E>1 MeV) is the neutron fluence in the vessel wall determined as follows (USNRC 1988) :

$$f = f_{surf}\, e^{-0.24a} \tag{5}$$

where f_{surf} represents the neutron fluence at the wetted inner surface of the vessel at the location of the postulated defect and a (inch) is the depth into the vessel wall measured from the vessel inner surface. Two values of neutron fluence at the inner surface of the reactor vessel are postulated and RT_{NDT} s at the crack tip locations are calculated as shown in Table 3.

Two cooling and heating rates of 100 °F/hr and 50 °F/hr are assumed and total number of analytical cases is 16 as shown in Table 2.

2.3 Determination of allowable pressure

The requirement to be satisfied and from which the allowable pressure for an assumed rate of

Table 3 Neutron fluence and RT_{NDT} at specified defect depth

Defect		Defect thickness (inch)	Physical defect depth (inch)	Neutron fluence ($\times 10^{19}$ n/cm^2)		RT_{NDT} at defect tip (°F)
a/t	surface			at inner surface	at defect tip	
1/4	inside	0	1.6250	3	2.0312	288.7
1/4	inside	0.125	1.7500	6	3.9423	321.2
1/4	inside	0.125	1.7500	3	1.9711	287.1
3/4	outside	0	1.6250	3	0.9311	245.3
3/4	outside	0.125	1.6250	6	1.8072	282.4
3/4	outside	0.125	1.6250	3	0.9036	243.6

temperature change throughout the life of the component at each temperature (ASME 1998a, 1998b) can be determined is :

$$2K_{Im} + K_{It} < K_{IR} \tag{6}$$

where K_{Im} and K_{It} are the stress intensity factors corresponding to membrane tension and a radial thermal gradient, respectively, and a factor of 2 is applied to the calculated K_{Im} values produced by primary stresses. This procedure is based on the principles of linear elastic fracture mechanics.

In this analysis, no margins due to instrument error are assumed, which is in general taken as –60 psig and +10 °F for pressure and temperature, respectively.

3. Analysis

3.1 Temperature distribution

Since the radius of curvature for the reactor vessel is very large when compared to the thickness, slab solution for the temperature distribution may be applied. The temperature distribution in the vessel wall $T(r,\ t)$ with uniform fluid temperature is assumed to be governed by the ordinary differential equation (Oezisik 1980) as follows :

$$\rho c T_t - k\left(\frac{1}{r}T_r + T_{rr}\right) = 0 \tag{7}$$

with the initial condition and boundary conditions given by

$$T(r, 0) = T_0 \tag{8}$$

$$T_r(r_0, t) = 0 \tag{9}$$

$$-kT_r(r_i, t) = h[T_c(t) - T(r_i, t)] \tag{10}$$

where T_0 is the initial coolant temperature, T_c the coolant temperature, k the heat conductivity of the material, h the heat transfer coefficient between the coolant and the vessel material, ρ the material density, c the material specific heat, r_o the outer radius, r_i the inner radius and t the time. Subscripts r and t represent the differentiation with respect to radial coordinate and time, respectively.

The finite difference equations for N radial points, at distance Δr apart, across the cross section of the vessel are expressed as follows (Myers 1971) :

for n =1

$$T_1^{t+\Delta t} = \left[1 - \frac{\Delta t \cdot k}{\rho c(\Delta r)^2}\left(1 + \frac{\Delta r}{r_1}\right) - \frac{\Delta t \cdot h}{\rho c \Delta r}\right]T_1^t + \frac{\Delta t \cdot k}{\rho c(\Delta r)^2}\left[\left(1 + \frac{\Delta r}{r_1}\right)T_2^t + \frac{\Delta r \cdot h}{k}T_c^t\right] \tag{11}$$

for $1 < n < N$

$$T_n^{t+\Delta t} = \left[1 - \frac{\Delta t \cdot k}{\rho c(\Delta r)^2}\left(2 + \frac{\Delta r}{r_n}\right)\right]T_n^t + \frac{\Delta t \cdot k}{\rho c(\Delta r)^2}\left[\left(1 + \frac{\Delta r}{r_n}\right)T_{n+1}^t + T_{n-1}^t\right] \tag{12}$$

and for $n = N$

$$T_N^{t+\Delta t} = \left[1 - \frac{\Delta t \cdot k}{\rho c(\Delta r)^2}\right]T_N^t + \frac{\Delta t \cdot k}{\rho c(\Delta r)^2}T_{N-1}^t \tag{13}$$

For stability in the finite difference calculation, we must choose Δt for a given Δr that both the followings are satisfied not to violate the second law of thermodynamics.

$$\frac{\Delta t \cdot k}{\rho c(\Delta r)^2}\left(2 + \frac{\Delta r}{r_1}\right) \le 1, \qquad \frac{\Delta t \cdot k}{\rho c(\Delta r)^2}\left(1 + \frac{\Delta r}{r_1}\right) + \frac{\Delta t \cdot h}{\rho c(\Delta r)} \le 1 \tag{14}$$

The heat transfer coefficient h is calculated based on forced convection under turbulent flow conditions. The variables involved are the mean velocity of the fluid constant u, and the density ρ, specific heat at constant pressure c_p, viscosity μ, and thermal conductivity of the coolant k. Empirical relation for fully developed turbulent flow in smooth tubes is recommended by Holman (1981) as follows :

$$Nu_d = 0.023 Re_d^{0.8} Pr^n \tag{15}$$

where n = 0.4 for heating and 0.3 for cooling and Nu_d (= hd/k), Re_d (= $\rho ud/\mu$), Pr (= $c_p\mu/k$) are Nusselt number based on diameter, Reynolds number based on diameter and Prandtl number, respectively. For water coolant, allowance for the variations in physical properties with temperature may be made by Glasstone (1960) as follows :

$$h = 0.148\left(1 + \frac{T}{10^2} - \frac{T^2}{10^5}\right)\left(\frac{Q}{\rho A}\right)^{0.8}\frac{1}{D^{0.2}} \tag{16}$$

where $Q(lb_m/hr)$ is effective coolant flow rate, $A(\mathrm{ft}^2)$ effective flow area and D(ft) the equivalent hydraulic diameter of the coolant channel. The values for the heat transfer coefficient given by this relationship are in good agreement with those obtained from Eq. (15) for temperatures up to 600 °F.

3.2 Stress distribution

The thermal stress distribution $\sigma_T(r, t)$ at shell locations away from the ends is calculated using the following equations (Timoshenko and Goodier 1970) :

$$\sigma_{T,\,hoop}(r,\,t) \;=\; \frac{\beta E}{1-\nu}\left[\frac{1}{r^2}\int_{r_i}^{r} T(r,\,t)rdr - T(r,\,t) + \frac{1}{r^2}\frac{r^2+r_i^2}{r_o^2-r_i^2}\int_{r_i}^{r_o} T(r,\,t)rdr\right] \tag{17}$$

$$\sigma_{T,\,axial}(r,\,t) \;=\; \frac{\beta E}{1-\nu}\left[\frac{2}{r_o^2-r_i^2}\int_{r_i}^{r_o} T(r,\,t)rdr - T(r,\,t)\right] \tag{18}$$

where E is Young's modulus, β the coefficient of thermal expansion and ν the Poisson's ratio.

The stresses $\sigma_p(r,\ t)$ due to internal pressure p are calculated using the following equations (Timoshenko and Goodier 1970) :

$$\sigma_{p,\,hoop}(r,\,t) \;=\; p(t)\frac{r_i^2}{r_o^2-r_i^2}\times\frac{r_o^2+r^2}{r^2} \tag{19}$$

$$\sigma_{p,\,axial}(r,\,t) \;=\; p(t)\frac{r_i^2}{r_o^2-r_i^2} \tag{20}$$

3.3 Maximum postulated defect

In accordance with the ASME code Section III, the maximum postulated defect is a sharp, surface defect normal to the direction of maximum stress. Defects are postulated at both the inside and outside surfaces. For section thickness of 4 in. to 12 in., it has a depth of one-fourth of the section thickness and a length of 11½ times the section thickness. For sections greater than 12 in. thick, the postulated defect for the 12 in. section is used. For section less than 4 in. thick, the 1 in. deep defect is conservatively postulated as shown in Fig. 2.

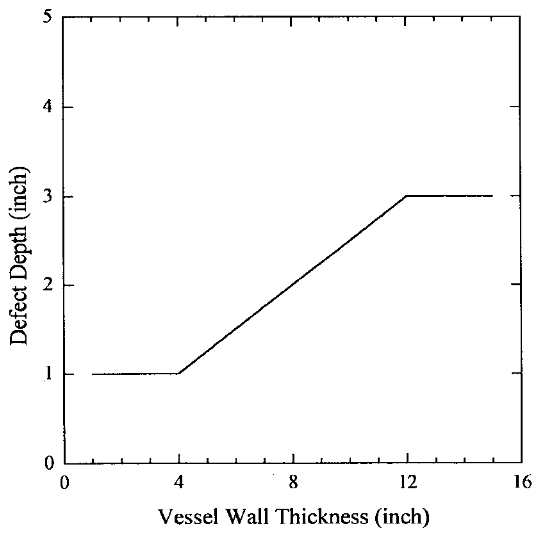

Fig. 2 Maximum postulated defect depth

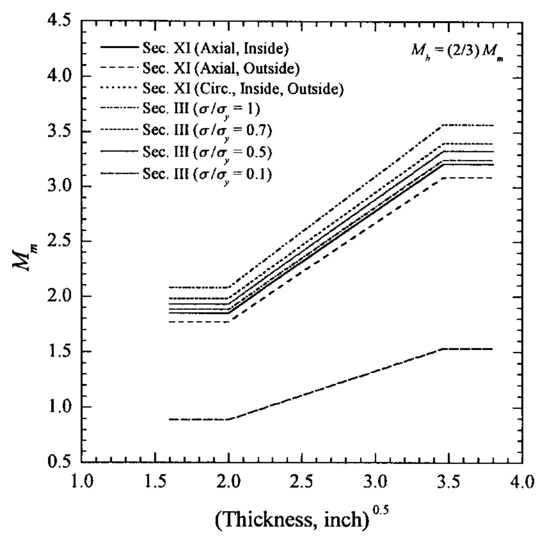

Fig. 3 Comparison of M_m from Appendix G between Section III and XI

3.4 Stress intensity factor

In ASME code Section III, the stress intensity factor K_I corresponding to membrane tension for the postulated defect is (ASME 1998a) :

$$K_{Im} = M_m \times \text{membrane stress} \tag{21}$$

where M_m is from Fig. G-2214-1 of Appendix G to ASME code Section III as shown in Fig. 3 (ASME 1998a). The K_I corresponding to bending stress for the postulated defect is :

$$K_{Ib} = M_b \times \text{maximum bending stress} \tag{22}$$

where M_b is two-thirds of the M_m as shown in Fig. 3. The K_{It} produced by thermal stress is calculated from the moment produced by the radial thermal gradient using Eqs. (17) or (18). In the similar fashion, the ASME code Section XI defines the stress intensity factors K_I corresponding to membrane tension for the postulated defect as (ASME 1998b) :

$$K_{Im} = M_m \times \frac{pr_i}{r_o - r_i} \tag{23}$$

where M_m is given according to the vessel wall thickness as shown in Table 4. The K_I corresponding to bending stress for the postulated axial and circumferential defect is obtained by Eq. (22). The maximum K_I produced by a radial thermal gradient for a postulated axial or circumferential inside surface defect is :

$$K_{It} = 0.953 \times 10^{-3} \times \text{CR} \times (r_o - r_i)^{2.5} \tag{24}$$

where CR is the cool-down rate in °F/hr, or K_I for a postulated axial or circumferential outside surface defect is :

$$K_{It} = 0.753 \times 10^{-3} \times \text{HU} \times (r_o - r_i)^{2.5} \tag{25}$$

where HU is the heat-up rate in °F/hr. Alternatively, the K_I can be calculated for any thermal distribution at any specified time for a 1/4-thickness axial or circumferential surface defect. For an inside surface defect during cool-down, the maximum K_I is :

$$K_{It} = (1.0359C_0 + 0.6322C_1 + 0.4753C_2 + 0.3855C_3)\sqrt{\pi a} \tag{26}$$

And for an outside surface defect during heat-up, the maximum K_I is :

$$K_{It} = (1.043C_0 + 0.630C_1 + 0.481C_2 + 0.401C_3)\sqrt{\pi a} \tag{27}$$

Table 4 M_m for surface defect

$\sqrt{\text{thickness, in}}$	Axial defect		Circumferential defect	
	inside	outside	inside	outside
$\sqrt{\text{thickness, in}} < 2$	1.85	1.77	0.89	0.89
$2 < \sqrt{\text{thickness, in}} < 3.464$	$0.926\times\sqrt{\text{thickness, in}}$	$0.893\times\sqrt{\text{thickness, in}}$	$0.443\times\sqrt{\text{thickness, in}}$	$0.443\times\sqrt{\text{thickness, in}}$
$3.464 < \sqrt{\text{thickness, in}}$	3.21	3.09	1.53	1.53

The coefficients C_0, C_1, C_2 and C_3 are determined from the thermal stress distribution at any specified time during the heat-up and cool-down using the following equation :

$$\sigma(x) = C_0 + C_1(x/a) + C_2(x/a)^2 + C_3(x/a)^3 \tag{28}$$

where x is a dummy variable that represents the radial distance from the appropriate surface and a is the maximum crack depth.

3.5 Allowable pressure by ASME code Section III

The radial stress distributions due to internal pressure and thermal gradient during heat-up are shown schematically in Fig. 4(a). Assuming a possible defect at the a/t = 1/4 location, the thermal stress tends to alleviate the pressure stress at this point in the vessel wall and, therefore, the steady state pressure stress would represent the maximum stress condition at a/t = 1/4 location. At the a/t = 3/4 location, the pressure stress and thermal stress add and, therefore, the combination for a given heat-up rate represents the maximum stress at the a/t = 3/4 location. The maximum overall stress between a/t = 1/4 and a/t = 3/4 location then determine the maximum allowable reactor pressure at the given coolant temperature (ASME 1998a).

The heat-up P-T limit curves are thus generated by calculating the maximum steady state pressure based on a possible defect at the a/t = 1/4 location from Eq. (29), which is obtained from Eqs. (6) and (19)

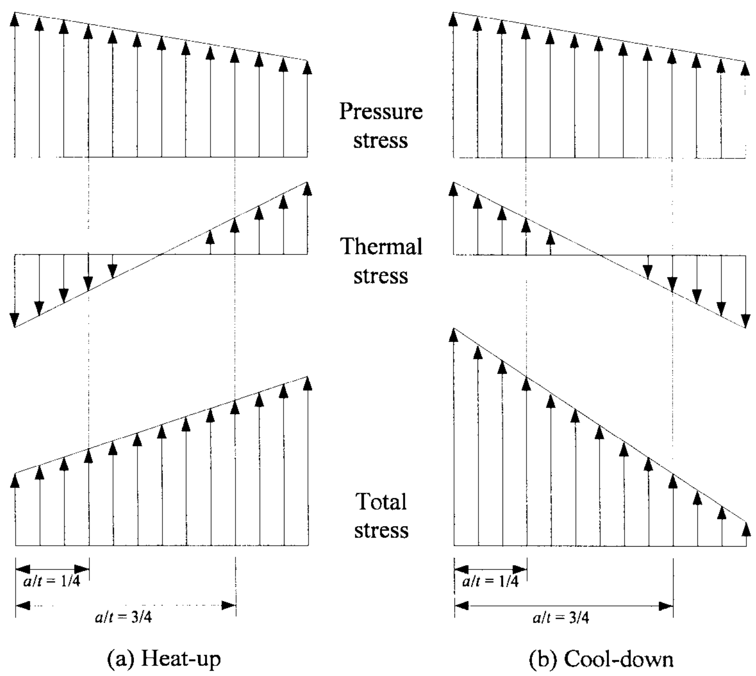

Fig. 4 Heat-up and cool-down stress distributions

$$p_{a/t\,=\,1/4} = \frac{K_{IR}}{2M_m} \cdot \frac{r_o^2 - r_i^2}{r_i^2} \cdot \frac{(r_o/4 + 3r_i/4)^2}{r_o^2 + (r_o/4 + 3r_i/4)^2} \tag{29}$$

where M_m is determined from the curves in Fig. 4 and K_{IR} is obtained from Eqs. (1) or (2) using the coolant temperature and RT_{NDT} at the a/t =1/4 location. At the a/t =3/4 location, the maximum pressure is determined as :

$$p_{a/t\,=\,3/4} = \frac{K_{IR} - K_{It}}{2M_m} \cdot \frac{r_o^2 - r_i^2}{r_i^2} \cdot \frac{(r_i/4 + 3r_o/4)^2}{r_o^2 + (r_i/4 + 3r_o/4)^2} \tag{30}$$

where K_{IR} is obtained from Eq. (1) or (2) using the material temperature and RT_{NDT} at the a/t =3/4 location. The minimum of these maximum allowable pressures at the given coolant temperature determines the maximum operation pressure.

During cool-down, the radial stress distributions due to internal pressure and thermal gradient are shown schematically in Fig. 4(b), which shows that the a/t = 1/4 location always controls the maximum stress since the thermal gradient produces tensile stresses at this location. Thus, the steady state pressure is the same as that given in Eq. (29). For each cool-down rate, the maximum pressure is evaluated at the a/t = 1/4 location from

$$p_{a/t\,=\,1/4} = \frac{K_{IR} - K_{It}}{2M_m} \cdot \frac{r_o^2 - r_i^2}{r_i^2} \cdot \frac{(r_o/4 + 3r_i/4)^2}{r_o^2 + (r_o/4 + 3r_i/4)^2} \tag{31}$$

where K_{IR} is obtained from Eq. (1) or (2) using the material temperature and RT_{NDT} at the a/t =1/4 location. The minimum of these maximum allowable pressures at the given coolant temperature determines the maximum operation pressure.

For the circumferential flaw, the maximum operation pressure is calculated in a similar method as described for the axial flaw.

3.6 Allowable pressure by ASME code Section XI

For the start-up condition, the allowable pressure-temperature relationship is the minimum pressure at any temperature determined from the calculated steady-state pressure resulting for the 1/4-thickness inside surface postulated defects as :

$$p = \frac{K_{IR}}{2M_m} \cdot \frac{r_o - r_i}{r_i} \tag{32}$$

and the calculated results from all beltline materilas for the heat-up stress intensity factors using the corresponding 1/4-thickness outside surface defects as :

$$p = \frac{K_{IR} - K_{It}}{2M_m} \cdot \frac{r_o - r_i}{r_i} \tag{33}$$

For the cool-down condition, the allowable pressure-temperature relationship is the minimum pressure at any temperature determined from all vessel beltline materials for the cool-down stress intensity actors using the corresponding 1/4-thickness inside surface defects and Eq. (33).

4. Results and discussion

Two analysis programs are developed for the generation of P-T limit curve using the procedures of ASME code Section III and Section XI. One is PPoRA (Program for Pressure-Temperature Limit Curve of Reactor Vessel by ASME Code Section III) and the other is RViES (Reactor Vessel Integrity Evaluation System) by ASME code Section XI. The results of these two programs for the specified problems are compared.

Thermal stress intensity factors for cool-down and heat-up are shown in Fig. 5 and maximum values for cool-down are shown in Table 5. By comparing C1, C2, and C3 with C5 and C6, clad-included case produced larger stress intensity factors by 5% comparing with without-clad case. This is the same for cooling rate of 50 °F/hr. Also the stress intensity factor for cooling rate of 100 °F/hr is about twice that of 50 °F/hr. For the heat-up case, thermal stress intensity factors show the same fashion with cool-down case.

When nuclear power plant is operated for longer time, reactor vessel is more irradiated by neutron fluence. Consequently, the neutron fluence at the inner surface of the vessel becomes larger. Nuetron fluences of 6×10^{19} n/cm^2 and 3×10^{19} n/cm^2 are assumed and their effects of neutron fluence on the P-T curve are shown in Fig. 6, which shows that the allowable area for operation is decreased by the increase of the neutron fluence. This indicates that it is better to reduce the neutron fluence than any other action taken to increase the operation area in the P-T limit curve. Also, it can be seen that the decrease of fluence has more effect on the high temperature and high pressure region.

Two toughness curves of K_{IA} and K_{IC} are used and their results are compared each other as shown in Fig. 7. The allowable area based on K_{IC} curve is significantly increased. This is a good example to show that choosing less conservative fracture toughness curve may give an operator enough margin for the operation of the plant. However, even though toughness curve of K_{IA} is known to be too

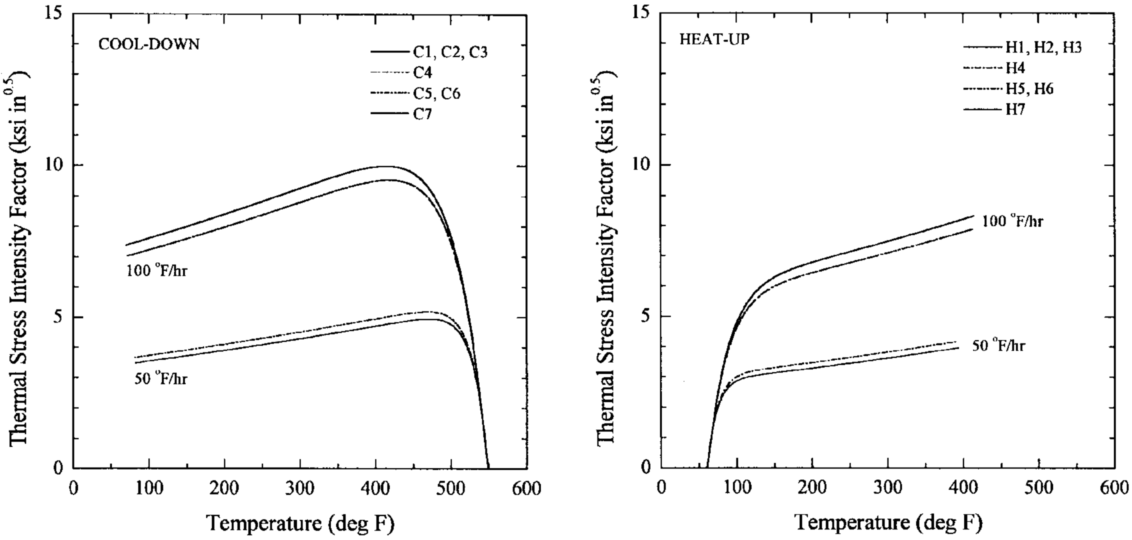

(a) Cool-down (b) Heat-up

Fig. 5 Thermal stress intensity factors for cool-down and heat-up

Table 5 Maximum thermal stress intensity factor for cool-down

Case	PPoRA		RViES		RViES		P-T Calculator	
	ASME Section III		ASME Section XI, Eq. (24)		ASME Section XI, Eq. (26)		Raju-Newman	
	K_I (ksi $\sqrt{\text{in}}$)	Temp. (°F)	K_I (ksi $\sqrt{\text{in}}$)	Temp. (°F)	K_I (ksi $\sqrt{\text{in}}$)	Temp. (°F)	K_I (ksi $\sqrt{\text{in}}$)	Temp. (°F)
C1	9.99	414						
C2	9.99	414						
C3	9.99	414						
C4	5.18	469						
C5	9.53	417	10.3	-	12.0	405	9.74	319
C6	9.53	417	10.3	-	12.0	405		
C7	4.94	471	5.13	-	6.25	464	4.91	429

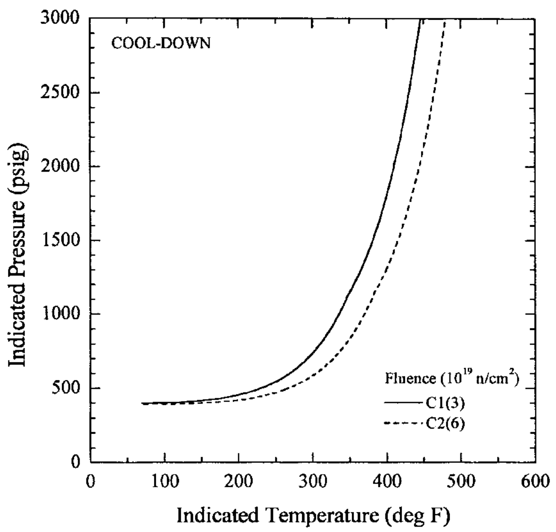

(a) Cool-down

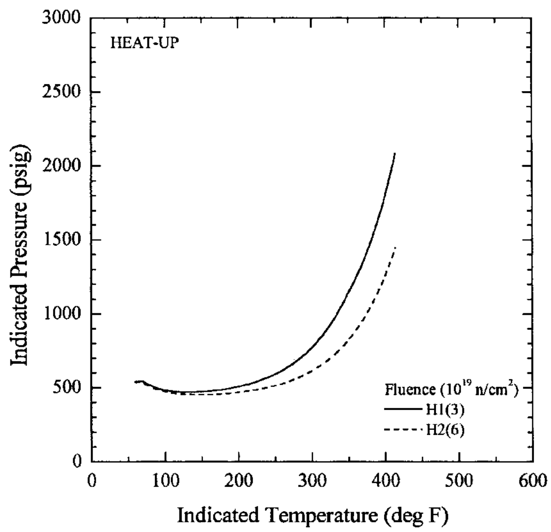

(b) Heat-up

Fig. 6 The effect of neutron fluence

conservative, the use of K_{IC} curve needs to be thoroughly reviewed and approved before application.

The effects of cooling or heating rate on the limit curve are shown in Fig. 8, where two different cooling or heating rates are used. Irrespective of the rates, the allowable operation area is the same for the first part of cooling procedure and for the last part of heating procedure for cooling and heating, respectively. And the only area affected with respect to the cooling or heating rate is the region of the lower pressure and lower temperature. In this case, lower cooling or heating rate, if accompanied by low neutron fluence, may give some benefit throughout the whole P-T limit curve.

P-T limit curves for with- and without-clad cases are shown in Fig. 9. The inclusion of clad generates almost the same limiting curve, which indicates that the difference is so small that the cladding effect on the curve is almost negligible. This is primarily associated with the very large reference flaw size assumed in this analysis of 1/4t which is large such that the crack tip is away

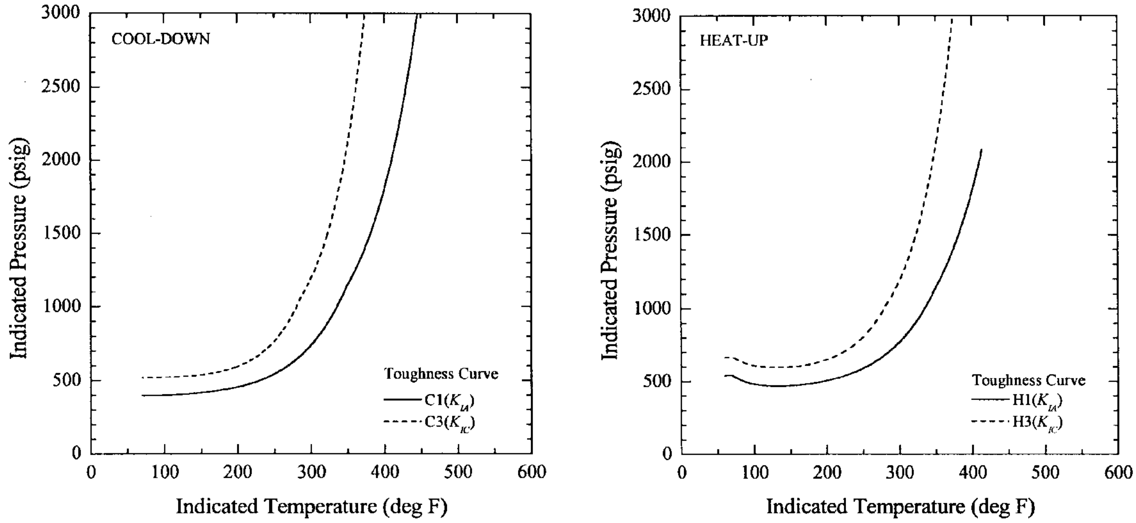

(a) Cool-down (b) Heat-up

Fig. 7 The effect of toughness curve

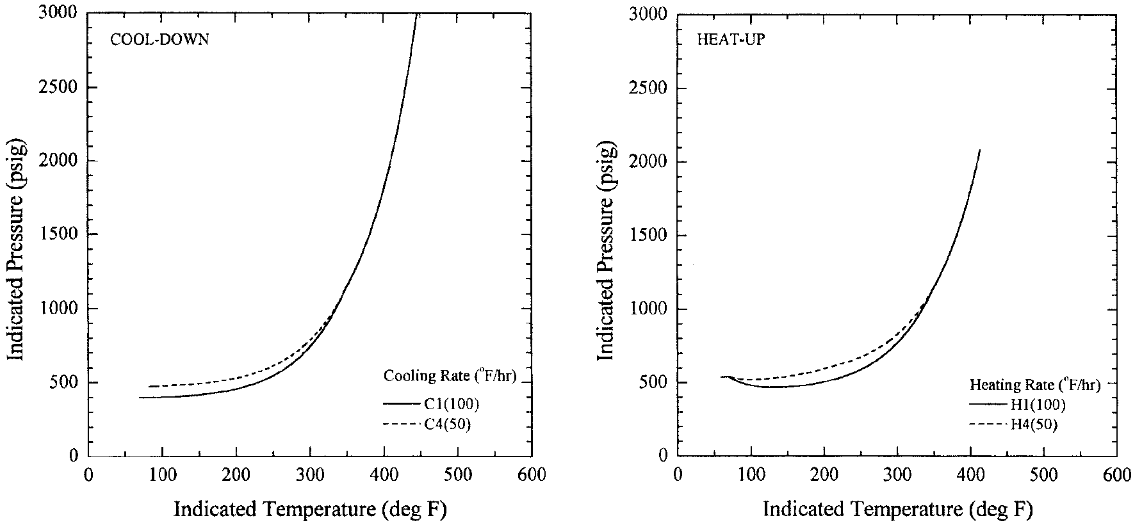

(a) Cool-down (b) Heat-up

Fig. 8 The effect of cooling and heating rate

from the vessel-clad interface. If the flaw size is reduced then cladding effect may be significant.

Fig. 10 shows the comparisons between defect orientations. The circumferential defect increased significantly the allowable operation area compared with axial defect. If the reactor vessel contains circumferential weld only and therefore circumferential defect is assumed, the P-T limit curves would not limit the start-up and shut-down procedure.

Thermal stress intensity factors for C5 and C7 are compared in Fig. 11 for three different

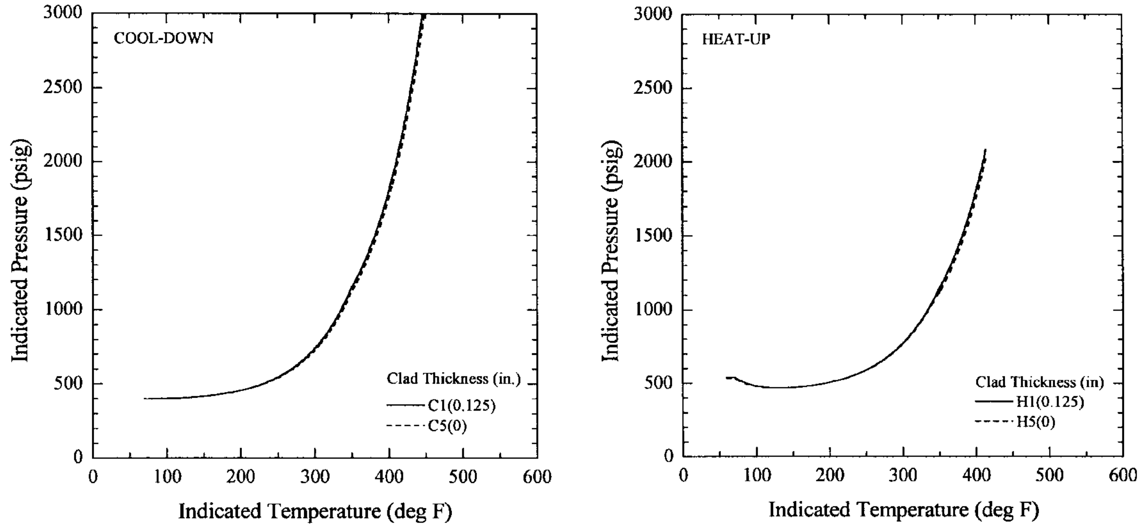

(a) Cool-down (b) Heat-up

Fig. 9 The effect of clad thickness

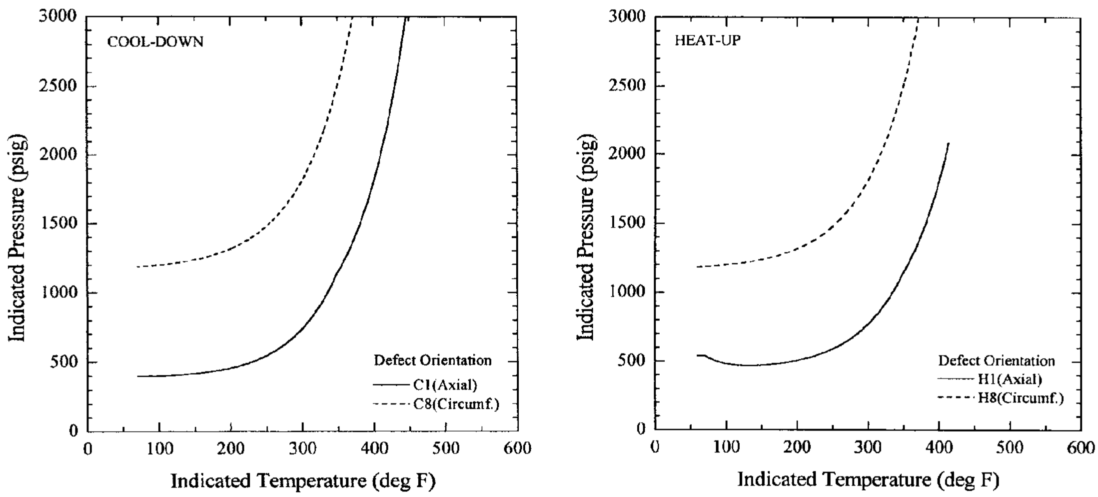

(a) Cool-down (b) Heat-up

Fig. 10 The effect of defect orientation

procedures described in Section III and Section XI of ASME code. In Section III, the moment produced by the radial thermal gradient is calculated and the equivalent linear stress is used for the maximum bending stress, resulting in the thermal stress intensity factors. In Section XI, two equations for the cool-down are used to calculate the thermal stress intensity factors. One is Eq. (24) which is independent on stress distribution. The other is Eq. (26) which varies with temperature. As shown in Fig. 11, Eq. (26) of Section XI gives the largest values followed by Eq. (24) of Section XI and Section III. However the difference of thermal stress intensity factors between Eqs. (24) and (26) has little effect on the P-T limit curves as shown in Fig. 12. Even though Eq. (26) has larger stress intensity factor than Eq. (24) by more than 15%, the P/-T limit curves are almost the same. This indicates that the allowable pressure determined by Eq. (33) has a function of (K_{IR} − K_{It}) which is also a function of temperature and stress intensity factor. Large thermal stress intensity factor means that it has a large temperature gradient and also high temperature at crack tip and high K_{IR}. Therefore, the value of (K_{IR} − K_{It}) is almost the same for two different thermal stress intensity factors. In comparing the curves by Section III and Section XI, it should be noted that Section III

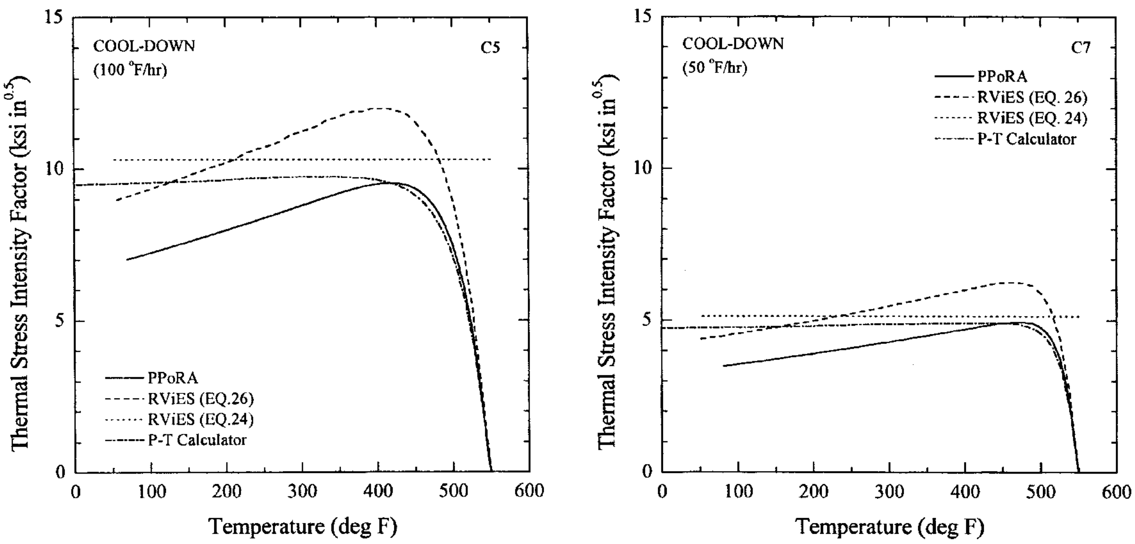

Fig. 11 Comparisons of thermal stress intensity factors for C5 and C7

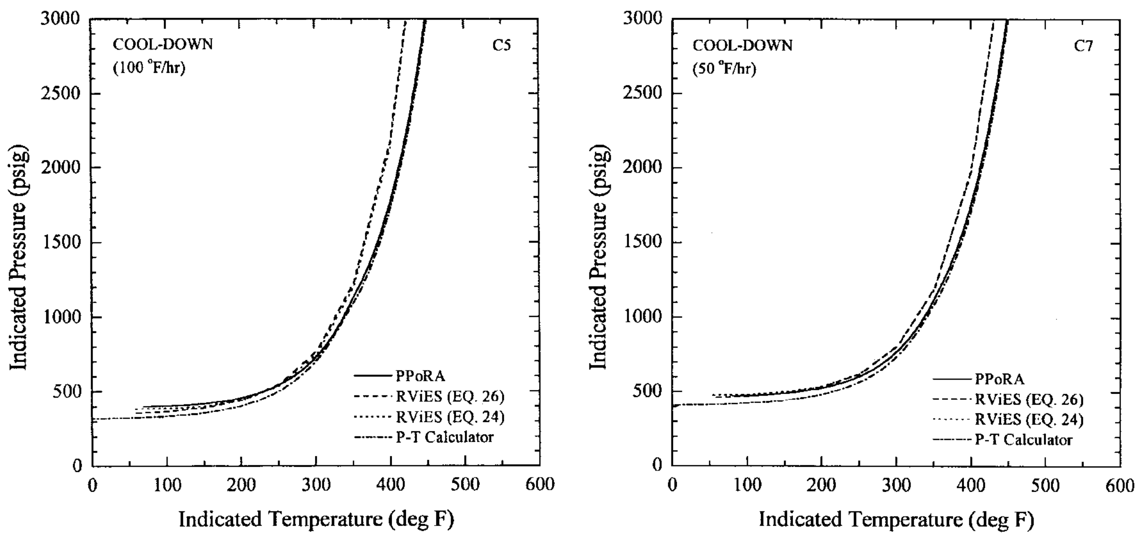

Fig. 12 Comparisons of P-T limit curves for C5 and C7

generates more conservative curves. This is due to the two reasons. One is the difference of M_m contained in Eqs. (29) through (33) to define allowable pressure. M_m between Section III and Section XI as shown in Fig. 3 shows that M_ms from Section III are always larger than those of Section XI, which indicates that Section III generates lower allowable pressure than Section XI. This is more severe if the ratio of stress to yield stress is considered to calculate M_m because Section XI does not consider yield stress for the calculation of M_m. The other factor is the equations used for the calculation of allowable pressure. During cool-down, allowable pressure is determined by Eqs. (31) and (33) for Section III and Section XI, respectively. Assuming that all values are the same except for geometry, the allowable pressures are calculated using r_o = 72.5 in. and r_i = 66 in. This gives about 3% higher allowable pressure in Section XI than that in Section III. The results of P-T Calculator developed by EPRI (1996) are also included in Figs. 11 and 12, which indicate that they represent the lower bound value and are closer to the results of Section III.

The effects of heat transfer coefficient are shown in Figs. 13 and 14, where three different constant values in addition to those by Eq. (16) are used for the temperature distribution followed by the calculation of stress intensity factors and finally P-T limit curves. Eq. (16) calculates the heat transfer coefficient (Btu/hr ft^2 °F) ranging from 4500 to 1700 depending on the coolant velocity and temperature, etc. Constant values of 5000, 3000 and 1000 are used to investigate the effect of the heat transfer coefficient on the thermal stress intensity factors. As shown in Fig. 13 there is no difference between them but care should be taken not to choose too low value below 1000. As expected, the resulting P-T limit curves as shown in Fig. 14 are not affected by the use of constant values of the heat transfer coefficient.

5. Conclusions

P-T limit curves are generated using the procedures of Appendix G to ASME code Section III and

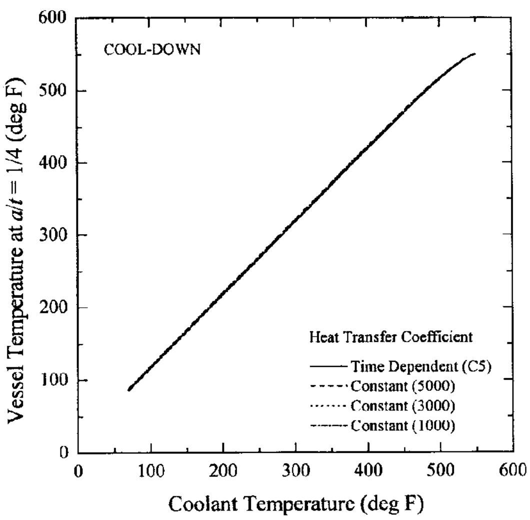

(a) Vessel temperature

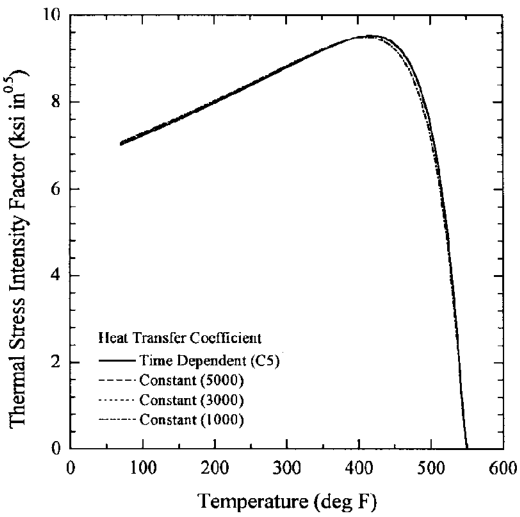

(b) Stress intensity factor

Fig. 13 The effect of heat transfer coefficient on temperature

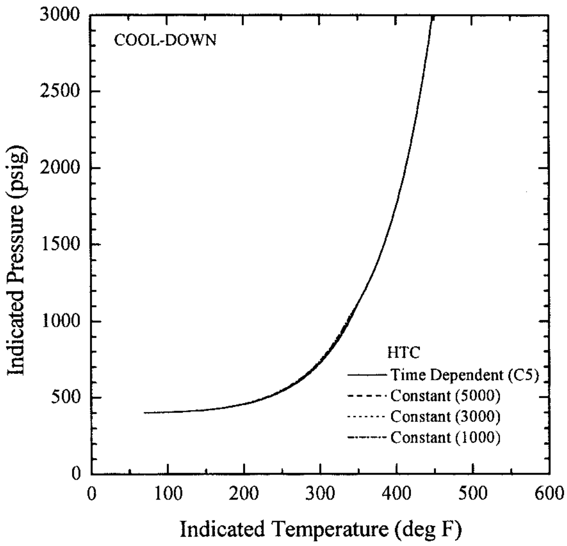

Fig. 14 The effect of heat transfer coefficient on P-T limit curve

Section XI. Eight different cases are postulated for cool-down or heat-up with respect to defect orientation, clad thickness, toughness curve, cooling or heating rate and neutron fluence. Their results are compared generating following conclusions:

1. Defect orientation and toughness curve are found to be the most important contributors to determine the P-T limit curve.
2. The cladding effects on the P-T limit curve are insignificant for the reference flaw size of 1/4*t*.
3. Neutron fluence and cooling or heating rate have some effect on the high and low pressure-temperature region, respectively. Therefore, the decrease of cooling or heating rate accompanied by the reduction of neutron fluence has some benefit throughout the P-T limit curve.
4. The operating window is increased dramatically by using K_{IC} as the reference toughness.
5. The selection of circumferential direction of defect orientation expanded significantly the allowable operating area for circumferential defect.

References

ASME. (1998a), *ASME Boiler and Pressure Vessel Code,* Section III Rules for Construction of Nuclear Power Plant Components, Appendix G Protection against Nonductile Failure, The American Society of Mechanical Engineers.

ASME. (1998b), *ASME Boiler and Pressure Vessel Code,* Section XI Rules for Inservice Inspection of Nuclear Power Plant Components, Appendix G Fracture Toughness Criteria for Protection against Failure, The American Society of Mechanical Engineers.

ASME. (1998c), *ASME Boiler and Pressure Vessel Code,* Section XI Code Case N-640, “Alternative reference fracture toughness for development of P-T limit curves”, The American Society of Mechanical Engineers.

EPRI. (1996), “P-T calculator for window Ver. 1.0”, Electric Power Research Institute.

Glasstone, G. (1960), *Principles of Nuclear Reactor Engineering,* D.Van Nostrand Co., New Jersey.

Holman, J.P. (1981), *Heat Transfer,* McGraw-Hill, London.

Myers, G.E. (1971), *Analytical Method in Conduction Heat Transfer*, McGraw-Hill, New York.
Oezisik, M.N. (1980), *Heat Conduction*, John Wiley & Sons, New York.
Timoshenko, S.P. and Goodier, J.M. (1970), *Theory of Elasticity*, McGraw-Hill, New York.
USNRC. (1988), "Radiation embrittlement of reactor vessel materials", Regulatory Guide 1.99, Rev.2, US Nuclear Regulatory Commission, May.
USNRC. (1996), "Fracture toughness requirements for protection against pressurized thermal shock events", 10 CFR 50.61, US Nuclear Regulatory Commission, May.

Notation

a : depth into the vessel wall
A : effective flow area
c : specific heat
c_p : specific heat at constant pressure
D : equivalent hydraulic diameter
E : Young's modulus
f : neutron fluence
h : heat transfer coefficient
k : heat conductivity
K_I : stress intensity factor
K_{IA} : crack arrest critical K_I
K_{IC} : static initiation critical K_I
K_{IR} : reference stress intensity factor
K_{Ib} : stress intensity factor corresponding to bending stress
K_{Im} : stress intensity factor corresponding to membrane tension
K_{It} : stress intensity factor corresponding to a radial thermal gradient
l : length of the defect
M_b : correction factor for bending stress
M_m : correction factor for membrane stress
Nu_d : Nusselt number based on diameter
Pr : Prandtl number
Q : effective coolant flow rate
r_i : inner radius
r_o : outer radius
Re_d : Reynolds number based on diameter
RT_{NDT} : reference nil ductility temperature
t : time
T : temperature
u : mean velocity of the fluid constant
β : coefficient of thermal expansion
μ : viscosity
ν : Poisson's ratio
ρ : density
σ : stress